

## Spin filtering through ferromagnetic BiMnO<sub>3</sub> tunnel barriers

M. Gajek,<sup>1,2</sup> M. Bibes,<sup>3</sup> A. Barthélémy,<sup>1,\*</sup> K. Bouzouane,<sup>1</sup> S. Fusil,<sup>1,4</sup> M. Varela,<sup>5</sup> J. Fontcuberta,<sup>2</sup> and A. Fert<sup>1</sup>

<sup>1</sup>Unité Mixte de Physique CNRS/Thales, Route Départementale 128 91767 Orsay, France

<sup>2</sup>Institut de Ciència de Materials de Barcelona, CSIC, Campus de la UAB, 08193 Bellaterra, Spain

<sup>3</sup>Institut d'Electronique Fondamentale, Université Paris-Sud, 91404 Orsay, France

<sup>4</sup>Université d'Evry, rue du Père Jarlan, 91025 Evry, France

<sup>5</sup>Departamento de Física Aplicada i Òptica, Universitat de Barcelona, Diagonal 647, 08028 Barcelona, Spain

(Received 19 April 2005; published 18 July 2005)

We report on experiments of spin filtering through ultrathin single-crystal layers of the insulating and ferromagnetic oxide BiMnO<sub>3</sub> (BMO). The spin polarization of the electrons tunneling from a gold electrode through BMO is analyzed with a counterelectrode of the half-metallic oxide La<sub>2/3</sub>Sr<sub>1/3</sub>MnO<sub>3</sub> (LSMO). At 3 K we find a 50% change of the tunnel resistances according to whether the magnetizations of BMO and LSMO are parallel or opposite. This effect corresponds to a spin-filtering efficiency of up to 22%. Our results thus show the potential of complex ferromagnetic insulating oxides for spin filtering and injection.

DOI: 10.1103/PhysRevB.72.020406

PACS number(s): 75.47.Lx, 79.60.Jv, 85.75.-d

Obtaining highly spin-polarized electron tunneling is an important challenge nowadays in spintronics, either for spin injection into semiconductors<sup>1,2</sup> or for magnetoresistive effects.<sup>3</sup> The classical way is by tunneling from a ferromagnetic conductor through a nonmagnetic barrier. This is the basic mechanism of the tunneling magnetoresistance (TMR) of tunnel junctions composed of two ferromagnetic electrodes (spin emitter and spin analyzer) separated by a nonmagnetic insulator.<sup>4</sup> Such tunnel junctions are currently applied to the development of sensors and memories; magnetic random access memories (MRAM). Spin-polarized tunneling from a ferromagnetic metal through a nonmagnetic layer is also what can be used for spin injection into a semiconductor.<sup>5</sup> Another way for spin-polarized tunneling has been little explored: this is tunneling from a nonmagnetic electrode through a ferromagnetic insulator. The concept was reported by Moodera *et al.*<sup>6</sup> with EuS tunnel barriers. The effective barrier height of an insulating layer corresponds to the energy difference between the Fermi level and the bottom of the conduction band (or the top of the valence band). A spin-dependent barrier height is therefore expected from the spin splitting of the energy bands in a ferromagnetic insulator. The exponential dependence of the tunneling on the barrier height can lead to a very efficient spin filtering. This has been confirmed, at least at low temperature, by the very high spin polarizations obtained by tunneling through barriers of EuS and EuSe (Refs. 6 and 7) and more recently with EuO.<sup>8</sup> Spin-filtering tunnel barriers can be of high interest for spin injection into semiconductors without using ferromagnetic metals as spin-polarized injectors. Very large magnetoresistance effects can also be expected by switching from parallel to antiparallel the magnetic configuration of two spin filter barriers in a double junction.<sup>9</sup>

To demonstrate spin filtering by a ferromagnetic barrier, the spin polarization of the current tunneling from a nonmagnetic electrode can be analyzed either with a superconductor,<sup>6,7</sup> or with a ferromagnetic counterelectrode.<sup>10</sup> In the latter case, the ferromagnetic counterelectrode collects differently the spins parallel and antiparallel to its magnetization, so that the current depends on the

relative orientations of the magnetic moments of the ferromagnetic barrier and counterelectrode. This is illustrated by the experiments of LeClair *et al.*<sup>10</sup> with an Al electrode, an EuS barrier, and a counterelectrode of ferromagnetic Gd. A TMR of up to 130% at 2 K has been obtained with this type of tunnel junction.<sup>10</sup>

Previously, experiments of spin filtering by ferromagnetic barriers have been performed with insulating layers of Eu chalcogenides. However, the very low Curie temperature of EuS (16 K) or EuSe (4.6 K), and the poor chemical compatibility of the Eu chalcogenides with many possible electrode materials limit their practical potential for spin filtering. The list of other possible candidates includes a few ferromagnetic perovskite oxides and a large family of ferrites (spinel and garnets). Compared to the complex crystal structure of the ferrites, perovskites are relatively simple and more convenient for integration into tunnel heterostructures, particularly if an isostructural fully polarized half-metallic ferromagnetic metal, such as La<sub>2/3</sub>Sr<sub>1/3</sub>MnO<sub>3</sub> (LSMO) (Ref. 11) is used as a spin analyzer to probe the filter efficiency.

BiMnO<sub>3</sub> (BMO) is an insulating and ferromagnetic perovskite oxide, having a Curie temperature ( $T_C$ ) of 105 K and a magnetic moment of  $3.6\mu_B$ /formula unit (in bulk).<sup>12</sup> It is a highly insulating compound and, remarkably, the insulating state is very robust.<sup>12</sup> Experimental determinations of the exchange splitting of the (empty) conduction band of BMO have not been reported; however it can be estimated to about 0.5 eV from linear spin-density approximation (LSDA) calculations<sup>13</sup> and to 1.6 eV from LSDA+ $U$ .<sup>14</sup> In both cases, the gap is smaller for spin-up electrons, so that when used as a spin-filter barrier, a BMO layer should filter out spin-down electrons and produce a positively spin-polarized current. From the gap found by LSDA+ $U$ , a computation technique that is commonly accepted to be more reliable to calculate band gaps, it follows that the exchange splitting in BMO is larger than that predicted for EuS [0.36 eV (Ref. 15)] and EuO [0.6 eV (Ref. 16)], which should result in an increased spin-filtering efficiency. Therefore, both from the electronic point of view and from materials perspective, BMO appears

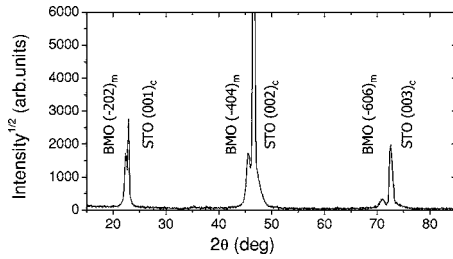


FIG. 1.  $\theta$ - $2\theta$  scan of a 30-nm film grown at 625 °C.

as an ideal perovskite to be implemented as a spin-filter barrier.

In this paper we report on the growth of thin epitaxial layers of the BiMnO<sub>3</sub> perovskite and their integration in spin-filter structures. We demonstrate the spin-filtering properties of tunnel barriers of BMO in Au-BMO-LSMO junctions. The device can be operated up to about 40 K. Our results demonstrate the potential of complex ferromagnetic oxides for high temperature spin filtering and spin injection.

BMO thin films were prepared on (001) SrTiO<sub>3</sub> (STO) substrates by pulsed laser deposition using a KrF excimer laser ( $\lambda=248$  nm). The growth of BMO was carried out from a nonstoichiometric multiphase target with a Bi:Mn ratio of 1.15, in an oxygen pressure of 0.1 mbar. Bulk BMO has a heavily distorted perovskite structure that can be represented in the monoclinic  $C2$  space group.<sup>17</sup> In the triclinic pseudocubic unit cell the lattice parameters are  $a=c=3.985$  Å,  $b=3.989$  Å with  $\alpha=\gamma=91.4^\circ$ ,  $\beta=91^\circ$ .<sup>17</sup> Extensive details on film growth and structural characterization will be reported elsewhere.<sup>18</sup> Here we just mention that single-phase BMO films have only been obtained in a narrow temperature window around 625 °C.

In Fig. 1 we show a  $\theta$ - $2\theta$  scan of a BMO film of nominal thickness 30 nm. Diffraction peaks occurring at slightly lower angles than the (00l)<sub>c</sub> reflections ( $c$ : pseudocubic representation) of the STO substrate are clearly visible and could be indexed as (0l0)<sub>c</sub> reflections of the BMO film. They correspond to (l0l)<sub>m</sub> in the monoclinic ( $m$ ) system. We do not detect (lll)<sub>m</sub> and (3lll)<sub>m</sub> reflections, as found by Moreira dos Santos *et al.*<sup>19</sup>  $\phi$  scans of the (111)<sub>c</sub> reflections of the BMO layer and STO substrate (not shown) indicate a cube-on-cube growth. The out-of-plane parameter ( $c$ ) deduced from the angular position of the (040)<sub>c</sub> reflection is 3.96 Å, close to the  $b$  parameter in bulk (3.989 Å). As  $c$  is inferior to the bulk parameter in spite of the compressive strain induced by the mismatch of -0.7% with the substrate, the reduction of the cell volume with respect to bulk is likely to be due to some Bi deficiency.

On Fig. 2, we plot the magnetization ( $M$ ) vs applied magnetic field ( $H$ ) for a 30-nm-thick BMO film after subtracting the diamagnetic contribution of the STO substrate. We observe a clear ferromagnetic behavior with a coercive field of 470 Oe measured in plane and out of plane, and a remanence of 62 emu/cm<sup>3</sup> with the field in plane and 29 emu/cm<sup>3</sup> out of plane. The shape of the magnetization loops indicates that the easy axis clearly lies in the film plane while the out-of-plane direction is a hard axis. The magnetization is not saturated even in a field of several teslas. It only reaches

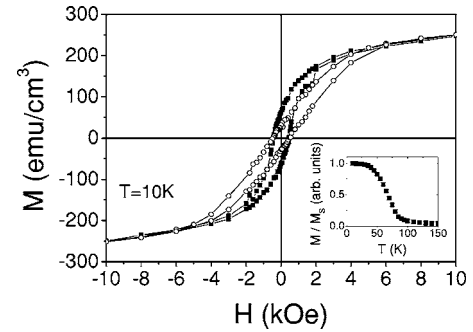


FIG. 2. Magnetization hysteresis cycles measured at 10 K with the field applied in plane (solid symbols) and out of plane (open symbols). Inset: the temperature dependence of the magnetization measured in a field of 1 kOe.

280 emu/cm<sup>3</sup> at 5 T, and is thus fairly reduced with respect to the bulk<sup>12</sup> [ $M(5\text{ T}) \approx 0.52M_{S\text{ bulk}}$ ], which is consistent with the results of Ohshima *et al.*<sup>20</sup> The slow increase of the magnetization at high field is likely to result from the progressive realignment of canted spins. Both the low magnetization and this canted behavior could be explained by the presence of Bi vacancies that locally disturb the complex orbital ordering essential for the long-range ferromagnetic order in BMO.<sup>21</sup> The temperature dependence of the magnetization of this 30-nm film (see inset of Fig. 2) indicates that the ferromagnetic transition occurs around 100 K, which is close to the bulk value ( $\sim 105$  K).

We have measured the temperature dependence of the resistivity of a 30-nm BMO film in the 150–300 K range and found a thermally activated behavior with a room-temperature resistivity of  $\rho_{300\text{ K}}=175$  Ω cm ( $\rho_{300\text{ K}}=20$  kΩ cm for bulk<sup>12</sup>) and an activation energy of  $E_a=239$  meV ( $E_a=262$  meV for bulk<sup>12</sup>). Below 150 K, the film resistance was exceedingly large to be measured with the available experimental set up. Using the room-temperature resistivity value and the activation energy we estimate the resistivity around  $T_C$  to about 5 GΩ cm. This is somewhat smaller than that of bulk BMO ceramics but similar to what is reported for Bi<sub>0.9</sub>Sr<sub>0.1</sub>MnO<sub>3</sub>.<sup>12</sup> This high value of the resistivity allows us to rule out any sizeable contribution from the “bulk” conductivity of the BMO layer to the current in the tunneling experiments we present below.

In order to probe the potential of BMO as a ferromagnetic barrier for spin filtering, ultrathin BMO films (3.5 nm) were grown onto a STO(1 nm)/LSMO(25 nm)//STO template. The intercalated 1 nm of STO layer is to magnetically decouple the BMO barrier from the LSMO electrode. One also knows that the half-metallic character of LSMO is conserved at the interface with STO.<sup>11,22</sup> Atomic force microscopy (AFM) images of this structure show a very smooth surface suitable for patterning the sample into tunnel junctions with the following structure: Au/BMO/STO/LSMO.

Small junctions ( $50 \times 50$  nm<sup>2</sup>) were patterned by a nanolithography process based on the indentation of thin resist by conductive-tip AFM, followed by the filling of the resulting hole with a sputtered Au layer.<sup>23</sup> In these experiments, the resistance of the LSMO bottom electrode was always small enough to ensure homogeneous current flow through the

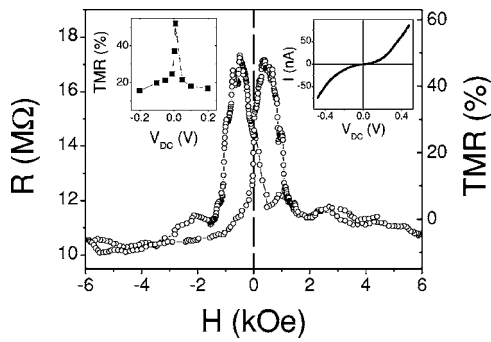


FIG. 3. Field dependence of the resistance of a junction at 3 K ( $V_{DC}=10$  mV). Insets: bias dependence of the TMR (left);  $I(V)$  curve of the junction (right).

junction. The  $I(V)$  curve of the right inset in Fig. 3 exhibits clearly the nonlinear and asymmetric behavior expected for tunnel junctions with different electrodes.

The  $R(H)$  plot of a Au/BMO/STO/LSMO junction in Fig. 3 is typical of TMR curves with a TMR of about 50%. The sharp increase of resistance at small field corresponds to the magnetic reversal of LSMO at its coercive field of about 100 Oe. The resistance drops back to its low-level value above 1.5 kOe, which is close to the value at which the magnetization cycle of the 30-nm BMO film closes (see Fig. 2). The resistance maximum corresponds to the antiparallel configuration of the magnetization of LSMO with the remanence of BMO ( $\sim 25\%$  of saturation). The slow and almost linear resistance variation at fields above 2 kOe is expected from the high-field susceptibility observed in the  $M(H)$  cycles (see Fig. 2). A part of this variation might also be due to reorientation of canted spins at the LSMO/STO interface.<sup>22</sup>

The positive value of the TMR is in agreement with the calculated band structure of BMO.<sup>13,14</sup> Using an extension of the Jullière model<sup>3</sup> ( $TMR=2P_1P_2/(1-P_1P_2)$ , where  $P_1=90\%$  is the typical spin polarization of LSMO at the interface with STO (Ref. 22), and  $P_2$  the spin polarization due to the BMO spin-filter effect), the measured TMR=50% corresponds to a spin-filter polarization of 22%. However, this value of the TMR is associated to the reversal of the LSMO magnetization with respect to the remnant magnetization of BMO, which amounts at only 25% of the saturation value. This indicates that a much higher polarization would be probably obtained for a BMO of higher remanence. One would expect a polarization of 88% for a remnant magnetization of 100%, which is close to the maximum spin-filter polarization found for EuS ( $\sim 85\%$ ),<sup>6</sup> but still lower than expected from the calculated value of the exchange splitting.

As shown in the inset (left) of Fig. 3, the TMR decreases at increasing bias. This feature is common in magnetic tunnel junctions<sup>24</sup> (MTJs) and ascribed in large part to magnon excitations at the electrode-barrier interfaces.<sup>25</sup> This mechanism is certainly also active here on the LSMO interface, but, since only one of the electrodes is magnetic, it cannot account for an approximately equal drop in positive and negative bias. A symmetric drop can only be due to magnon excitations *inside* the BMO barrier. With a tunneling current predominantly carried by electrons having a complex momentum component perpendicular to the layers and zero par-

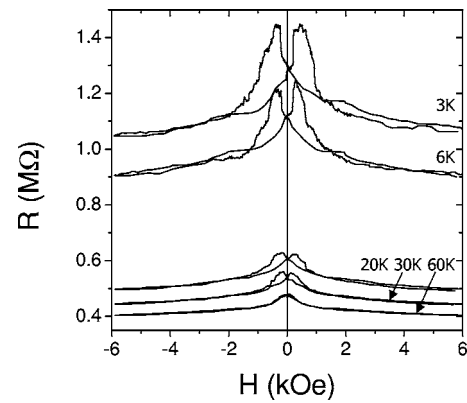


FIG. 4. Field dependence of the resistance at different temperatures for a second junction ( $V_{DC}=10$  mV).

allel component, excitations of magnons of parallel momentum can flip the spin of these electrons and scatter them into evanescent waves of different decay length. This can affect strongly the conductance and the TMR. Although this magnon contribution to the bias dependence of the TMR should be more important in spin filters than in conventional MTJs, they have not been incorporated in the existing spin-filter models,<sup>26</sup> and certainly deserves the attention of theorists.

In Fig. 4 we plot  $R(H)$  curves obtained for another Au/BMO/STO/LSMO junction at different temperatures. At 3 K, its resistance is somewhat lower than that of the junction of Fig. 3, which might be due to a slightly lower barrier thickness. The TMR of this junction is 29% at 3 K and then gradually decreases at increasing temperature. It can be noticed that the resistance of the junction decreases at increasing temperature. This is the usual variation for MTJs.<sup>27</sup> However, in the case of spin filtering by a ferromagnetic barrier, a contribution in the opposite directions is expected from the decrease of the spin splitting when  $T$  increases. Apparently the former contribution is predominant in our samples. Beyond 40 K, it remains only a small and reversible  $R(H)$  variation that should be predominantly due to spin canting reorientation. The temperature at which the spin-filter effect vanishes is thus lower than the Curie temperature of our 30-nm BMO films (see inset of Fig. 2). This may indicate that the  $T_C$  of BMO ultrathin layers is depressed compared to bulk value. Another possible explanation may be the progressive decrease of the coercive field of BMO as temperature increases. This decrease can be seen in the progressive narrowing of the magneto resistance peak between 3 and 60 K in Fig. 4 and is also confirmed by our magnetization measurements. The TMR of a magnetic tunnel junction is expected to vanish when the magnetizations of the two electrodes are reversed at about the same field.

In summary, we have grown single-phased thin films of the ferromagnetic insulator BiMnO<sub>3</sub> on (001)-oriented SrTiO<sub>3</sub> substrates. Spin filtering by a BMO tunnel barrier has been demonstrated by magnetotransport measurements on Au-BMO-LSMO junctions, which have shown up to 50% of TMR. The TMR decreases rapidly and symmetrically as a function of the bias voltage, which can be the signature of magnon excitations inside the magnetic barrier. This new inelastic scattering mechanism was not included in the

theory of spin-filter junctions<sup>26</sup> and has to be studied in more detail. Our results suggest that BMO could be used for spin injection into semiconductors as high-quality perovskite/Si (Ref. 28) and perovskite/GaAs (Ref. 29) structures have already been fabricated. Further work is needed to fully understand and improve the magnetic properties of BMO ultrathin film but this is the first experimental evidence of spin filtering with a complex oxide and thus constitutes a hallmark towards spinfilters operating at room temperature, using spinel ferrites for instance. In addition, since BMO is also ferroelectric,<sup>30</sup> and as a coupling between the magnetic and

dielectric properties in this material has been recently reported,<sup>31</sup> our experiment can be thought as a preliminary stage in the exploitation of multiferroic materials in spintronics devices.

This work has been supported in part by the MCyT (Spain) projects MAT2002-03431, FEDER, the Franco-Spanish project HF-20020090 and the E.U. STREP “Nanotemplates” (contract number NMPA4-2004-505955). M.G. acknowledges financial support from ICMA, through the Marie Curie Training Site program.

---

\*Electronic address: agnes.barthelemy@thalesgroup.com

- <sup>1</sup>E. I. Rashba, Phys. Rev. B **62**, R16267 (2000).
- <sup>2</sup>A. Fert and H. Jaffrès, Phys. Rev. B **64**, 184420 (2001).
- <sup>3</sup>M. Jullière, Phys. Lett. **54A**, 225 (1975).
- <sup>4</sup>J. S. Moodera, L. R. Kinder, T. M. Wong, and R. Meservey, Phys. Rev. Lett. **74**, 3273 (1995).
- <sup>5</sup>V. F. Motsnyi *et al.*, Phys. Rev. B **68**, 245319 (2003).
- <sup>6</sup>J. S. Moodera, X. Hao, G. A. Gibson, and R. Meservey, Phys. Rev. Lett. **61**, 637 (1988).
- <sup>7</sup>J. S. Moodera, R. Meservey, and X. Hao, Phys. Rev. Lett. **70**, 853 (1993).
- <sup>8</sup>T. S. Santos and J. S. Moodera, Phys. Rev. B **69**, 241203(R) (2004).
- <sup>9</sup>D. C. Worledge and T. H. Geballe, J. Appl. Phys. **88**, 5277 (2000).
- <sup>10</sup>P. LeClair *et al.*, Appl. Phys. Lett. **80**, 625 (2002).
- <sup>11</sup>M. Bowen *et al.*, Appl. Phys. Lett. **82**, 233 (2003).
- <sup>12</sup>H. Chiba, T. Atou, and Y. Syono, J. Solid State Chem. **132**, 139 (1997).
- <sup>13</sup>N. A. Hill and K. M. Rabe, Phys. Rev. B **59**, 8759 (1999).
- <sup>14</sup>T. Shishidou, N. Mikamo, Y. Uratani, F. Ishii, and T. Oguchi, J. Phys.: Condens. Matter **16**, S5677 (2004).
- <sup>15</sup>P. Wachter, *Handbook on the Physics and Chemistry of Rare Earths*, edited by K. A. Schneider and L. Eyring (North-Holland, New York, 1979), Vol. 2, 507.
- <sup>16</sup>P. G. Steeneken *et al.*, Phys. Rev. Lett. **88**, 047201 (2002).
- <sup>17</sup>T. Atou, H. Chiba, K. Ohoyama, Y. Yamaguchi, and Y. Syono, J. Solid State Chem. **145**, 639 (1999).
- <sup>18</sup>M. Gajek *et al.*, (unpublished).
- <sup>19</sup>A. F. Moreira dos Santos *et al.* Appl. Phys. Lett. **84**, 91 (2004).
- <sup>20</sup>E. Ohshima, Y. Saya, M. Nantoh, and M. Kawai, Solid State Commun. **116**, 73 (2000).
- <sup>21</sup>A. F. Moreira dos Santos *et al.*, Phys. Rev. B **66**, 064425 (2002).
- <sup>22</sup>V. Garcia *et al.*, Phys. Rev. B **69**, 052403 (2004).
- <sup>23</sup>K. Bouzehouane *et al.*, Nano Lett. **3**, 1599 (2003).
- <sup>24</sup>X.-F. Han *et al.*, Phys. Rev. B **63**, 224404 (2001).
- <sup>25</sup>S. Zhang, P. M. Levy, A. C. Marley and S. S. P. Parkin, Phys. Rev. Lett. **79**, 3744 (1997).
- <sup>26</sup>A. Saffarzadeh, J. Magn. Magn. Mater. **269**, 327 (2004).
- <sup>27</sup>C. H. Shang, J. Nowak, R. Jansen, and J. S. Moodera, Phys. Rev. B **58**, R2917 (1998).
- <sup>28</sup>R. A. McKee, F. J. Walker, and M. F. Chisholm, Phys. Rev. Lett. **81**, 3014 (1998).
- <sup>29</sup>Y. Liang *et al.*, Appl. Phys. Lett. **85**, 1217 (2004).
- <sup>30</sup>J. Y. Son, B. G. Kim, C. H. Kim, and J. H. Cho, Appl. Phys. Lett. **84**, 4971 (2004).
- <sup>31</sup>T. Kimura *et al.*, Phys. Rev. B **67**, 180401(R) (2003).